

# A model for cytoplasmic rheology consistent with magnetic twisting cytometry

J.P. Butler and S.M. Kelly

*Physiology Program, Harvard School of Public Health, Boston, MA, USA*

Received 26 March 1998; accepted in revised form 10 August 1998

---

## Abstract

Magnetic twisting cytometry is gaining wide applicability as a tool for the investigation of the rheological properties of cells and the mechanical properties of receptor-cytoskeletal interactions. Current technology involves the application and release of magnetically induced torques on small magnetic particles bound to or inside cells, with measurements of the resulting angular rotation of the particles. The properties of purely elastic or purely viscous materials can be determined by the angular strain and strain rate, respectively. However, the cytoskeleton and its linkage to cell surface receptors display elastic, viscous, and even plastic deformation, and the simultaneous characterization of these properties using only elastic or viscous models is internally inconsistent. Data interpretation is complicated by the fact that in current technology, the applied torques are not constant in time, but decrease as the particles rotate. This paper describes an internally consistent model consisting of a parallel viscoplastic element in series with a parallel viscoelastic element, and one approach to quantitative parameter evaluation. The unified model reproduces all essential features seen in data obtained from a wide variety of cell populations, and contains the pure elastic, viscoelastic, and viscous cases as subsets.

*Keywords:* Magnetic twisting cytometry; cell rheology; elasticity; stiffness; viscosity; plasticity; cytoskeleton

---

## 1. Introduction

### *1.1. Biological importance of rheology*

The rheological properties of cells are an important determinant of their intrinsic motions and of a wide variety of cell responses to mechanical stresses. The intrinsic motions include cell motility (Valberg, 1984), cell spreading (Wang and Ingber, 1995), and phagocytosis

---

Reprint requests to: Dr J.P. Butler, Physiology Program, Harvard School of Public Health, 665 Huntington Ave., Boston, MA 02115, USA; Tel.: 617-432-1662; Fax: 617-432-3468

in macrophages (Bizal et al., 1991). Responses to externally imposed mechanical stresses include the nature of deformation and sequestration of leukocytes in the circulation (Lien et al., 1991; Worthen et al., 1989), secretion of surfactant by Type II pneumocytes (Wirtz and Dobbs, 1990) and of NO by endothelial cells (Lamontagne et al., 1992). This category of responses also includes changes in the levels of some second messengers in response to mechanical perturbations of integrin receptors at the cell surface (Fong, 1996). One common feature linking rheological properties and mechanical function is the cytoskeleton. Selective disruption of filaments has enabled the partial assessment of the role that individual cytoskeletal filament systems play in determining intracellular properties (Tagawa et al., 1997; Valberg and Albertini, 1985; Valberg and Butler, 1990; Wang et al., 1993; Wang and Ingber, 1994). More recently, the importance of the mechanical linkages between the cytoskeleton and membrane bound receptors and the extracellular matrix is beginning to be appreciated (Wang et al., 1993; Wang and Ingber, 1994).

### *1.2. Magnetic twisting cytometry*

Magnetic twisting cytometry is an important tool by which rheological properties can be studied (Valberg and Butler, 1987; Valberg and Albertini, 1985; Valberg and Butler, 1990; Valberg and Feldman, 1987; Wang et al., 1993). The essence of this technology is found in the behavior of small ferromagnetic beads, placed intracellularly either through phagocytosis or injection, or bound to the cell membrane by coupling of ligand-coated beads to specific cell membrane receptors. It is important to recognize the several senses of averaging involved in the magnetic particle probe.

First, there is heterogeneity in size and shape of the particles themselves. For roughly spherical particles that are internalized, this is probably a minor issue, since the response is approximately independent of particle size (Valberg and Butler, 1987). The effect of heterogeneity with surface bound particles is not known.

Second, the physical location within or on the cell will be distributed, and therefore the mechanical properties of the adjacent milieu will be distributed as well.

Finally, the measurements are made on populations of cells which themselves may exhibit heterogeneous rheological properties. The final results are an average over all of these sources of variability.

Magnetized beads are rotated by a torque generated by a weak external magnetic field. The magnitude of the applied specific torque (torque per unit volume) and resulting angular rotation of the beads can be measured. The relationships between torque and angular rotation obtained as a function of time and twisting field strength are the primary data from which one attempts to obtain certain rheological properties. While these primary data are relatively\* straightforward, the characterization of these data in terms of specific parameters such as an elastic modulus (or stiffness) and a viscosity presents serious difficulties in interpretation; current methods for analyzing these data are not self-consistent.

### *1.3. The inconsistency*

At any given time during the application of the applied torque, the angular rotation and rotation rate may be supported by any combination of the cells' intrinsic elastic, viscous,

and even plastic properties. Current methodology defines the ratio of initial specific torque to rotational angle after 1 min or actual specific torque at 1 min to rotational angle after 1 min to be the sample “stiffness” (Zaner and Valberg, 1989; Valberg and Butler, 1990; Wang et al. 1993). This simple ratio in fact fails to characterize the cells’ actual stiffness, insofar as both yielding deformations as well as viscous contributions can masquerade as stiffness thus defined. This ratio is thus not equivalent to an “apparent” or “dynamic” stiffness in the sense of, e.g., the slope of an elliptical force/displacement loop with sinusoidal forcing. In particular, the notion of stiffness itself does not admit a lack of angular recovery following the cessation of bead twisting, a significant and very common observation in living cells. Similarly, in the quantification of viscosity, the use of strain rate cannot be simply related to the applied specific torque, if the torque is in large measure supported by elastic forces. In other words, the cross-talk among elastic, viscous, and plastic forces makes current methods of quantification internally inconsistent. This issue has been recognized (Bizal et al., 1991; Valberg and Butler, 1990) but to date there has been no systematic and self-consistent approach to the simultaneous estimation of these rheological properties of cells. It is the purpose of this article to present a model for intracellular rheology that can be used to estimate certain elastic, viscous, and plastic moduli, and that is consistent with much of the magnetometric data observed.

## 2. Technological Methods

Here we briefly summarize the essentials of the specific technical methodology used in magnetic twisting cytometry, discussed elsewhere at length (Valberg and Butler, 1987; Valberg and Feldman, 1987). First, ferromagnetic beads of roughly spherical shape, either within the cell or bound to receptors on the cell surface, are magnetized by a short but strong magnetic pulse. Second, a weak uniform “twisting” field  $B_{tw}$  is applied orthogonally to the original magnetization direction. This creates a torque on the particles which causes them to rotate. Third, the twisting field is turned off, and the cell-bead preparation is allowed to recover.

A magnetometer placed near the cells measures the component  $B(t)$  of the magnetic field in the direction of the original magnetization (the so-called remanent field) as a function of time  $t$ . As the particles rotate away from that initial direction due to the applied torque, this component decreases; let  $B_0$  be the field measured in the direction of the initial magnetization at time zero, then

$$B(t) = B \sin(\vartheta),$$

where  $\sin(\vartheta)$  is the average value of the sine of each particle’s angle of orientation measured from the direction of the twisting field. (Thus,  $\vartheta$  is a kind of average angle for the particles, but is not the simple mean angle. Furthermore, there are problems with the interpretation of  $\vartheta$  when intrinsic relaxation is present; see Section 6.) Here  $\vartheta = \pi/2$  corresponds to the initial magnetization direction and  $\vartheta = 0$  to the direction of the twisting field. Note that the extent of rotation is then  $\pi/2 - \vartheta$ . The bead angle is inferred from the measurement of  $B(t)$ ;

$$\vartheta(t) = \sin^{-1}(B(t)/B_0). \quad (1)$$

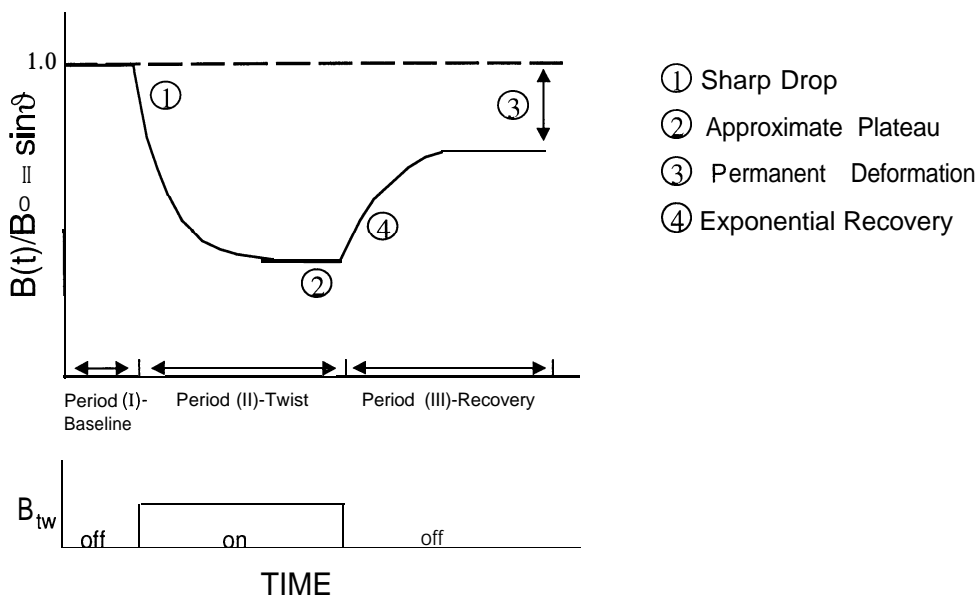


Fig. 1. Illustration of remanent magnetic field  $B(t)$  normalized by  $B_0$  (upper panel) and twisting field  $B_{tw}$  (lower panel) as a function of time during a single twist and recovery. Note that normalized remanent magnetic field can also be read as  $\sin(\vartheta)$ , where  $\vartheta$  is the angle between the magnetic moment of the particle and the direction of  $B_{tw}$ . (In particular, the initial  $\vartheta$  is  $n/2$ .) The three periods of the twist protocol are identified in the upper panel. Essential features of the data curve are indicated by the circled numbers.

The applied torque is equal to the cross product of the magnetic moment of the bead and the applied field. Thus the magnitude of the specific torque (torque per unit bead volume) at time  $t$ , denoted by  $T(t)$  is given by

$$T(t) = c B_{tw} \sin(\vartheta) = c B_{tw} B(t) / B_0, \quad (2)$$

where  $c$  is equal to the remanent magnetic moment per unit volume of particle, corrected by a shape factor to take into account any lack of sphericity of the particles. If  $c$  is known, then one can magnetometrically determine both the rotation of the particles (Eq. (1)), and the 'specific torque' (Eq. (2)), each as a function of time. It is important to recognize that while the applied field  $B_{tw}$  is a step function during the twisting procedure, the applied torque is not; by Eq. (2)  $T$  is time dependent in a manner dependent on the cells' response. It follows that a simple interpretation of these data by Fourier decomposition of an applied step cannot be done.

Since inertial effects are negligible,  $T$  must be equal to the specific torque conferred by the cell. This may be associated with some combination of the deformation (elastic or plastic) or deformation rate (viscosity). These observations lead to a simple method for calibrating the bead constant  $c$ . In particular,  $c$  can be easily determined for a given particle type by twisting the particles in fluid standards of known viscosity  $\mu$ .  $c$  is estimated, in effect, by the ratio of  $\mu(d\vartheta/dt)$  to  $B_{tw}B/B_0$  (Wang and Ingber, 1995; Zaner and Valberg, 1989).

The experimental protocol is divided into three periods (Fig. 1). Period I—Baseline is the interval between the initial magnetization and the initiation of the twisting field. Period II—

Twist is the typically one minute period when  $B_{tw}$  is on. Period III-Recovery is the one minute or longer period when  $B_{tw}$  has been turned off.

### 3. Theory

The apportioning of the net stress (Eq. (2)) and net strain (Eq. (1)) requires some kind of model structure for the underlying rheological elements. There are two extreme cases which illustrate this problem. (A) To the extent that there are different elements mechanically in parallel, their angular displacements will be equal and their contributions to stress will be additive. In that case, one can attribute the measurement of particle orientation or angular rotation (Eq. (1)) to these elements, but without a specific model one cannot attribute the measured stress unambiguously to any of the individual elements. (B) To the extent that there are different elements mechanically in series, their stresses will be equal but their angular displacements will be additive. In this case, the stress measurements (Eq. (2)) can be applied to the individual elements, but one cannot assign the angular displacements unambiguously.

If there is full angular recovery following the twist, this may be characterized by a class of models with no internal mechanical degrees of freedom. In such cases, the angular rotation and the specific torque measured by Eqs. (1) and (2) may suffice for the adequate characterization of the rheological properties of the cells. In sharp contrast, the observation of a significant amount of irreversible deformation or lack of full angular recovery implies, with few exceptions, the requirement of internal degrees of freedom for angular displacement.

Our goal then is the identification of a parsimonious model for cytoplasmic or cytoskeletal rheology that avoids the internal inconsistencies of all current techniques for analyzing magnetic twisting cytometry data. Specifically, we seek a model that (1) approximately satisfies all the essential qualitative features of twisting curves, and (2) simultaneously incorporates data both from the periods when the twisting field is on as well as during recovery with the twisting field off. Figure 1 shows a typical curve of the remanent magnetic field as a function of time, which has a number of features common to most experimental observations. The following is a list of the most important of these.

*Feature (1).* When the twisting field is turned on (a step function), one observes a relatively sharp drop in  $B(t)/B_0$ , which, being equal to  $\sin(\vartheta)$ , implies an even sharper drop in  $\vartheta$  from its initial value of  $n/2$ .

*Feature (2).* By the end of one minute of twisting,  $B(t)/B_0$  appears to be decaying towards a kind of plateau. This is true for many cell types and for many interventions, but there are a number of cells that do not appear to show this behavior; our assumption that there will be an asymptotic plateau for an indefinitely prolonged twisting period is potentially violated in these cells, although we will see that one subset of our proposed model is self consistent even with no plateau.

*Feature (3).* When the twisting field is turned off, there is a relatively sharp rebound or recovery of  $\vartheta(t)$  towards a final asymptote  $\vartheta_\infty$ .  $\vartheta_\infty$  is typically significantly less than  $n/2$ , indicating a loss of recovery, although some cell types and gel preparations show essentially complete recovery.

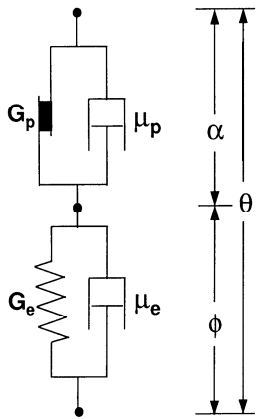


Fig. 2. Structure of the unified model which satisfies the essential features of the experimentally observed remanent magnetic field vs. time during twist and recovery. The model consists of a parallel viscoplastic element in series with a parallel viscoelastic element.  $G_p$  = yield stress;  $\mu_p$  = viscosity in parallel with  $G_p$ ;  $G_e$  = elastic modulus;  $\mu_e$  = viscosity in parallel with  $G_e$ . The angular displacements of the viscoplastic and viscoelastic elements are  $\alpha$  and  $\phi$ , respectively, with a total angular displacement given by  $\vartheta = \alpha + \phi$ .

*Feature (4).* The shape of  $\vartheta(t)$  over the entire experimental interval, comprising Period II—Twist together with Period III—Recovery, is not simply characterizable, but the shape of  $\vartheta(t)$  during Period III—Recovery by itself is approximately exponential.

The combined features listed above suffice to eliminate a large class of simple models with viscous, elastic, and plastic elements (e.g., a parallel viscoelastic material (Voigt body) always shows full recovery; a series viscoelastic material (Maxwell body) shows infinitely sharp jumps in angular displacement, etc.). Let  $x$  be an angular displacement of one of these elements (which may or may not be identified with the net angular displacement  $\pi/2 - \vartheta$ ). The specific torques  $T$ , when applied to these elements, satisfy the following: for viscous media  $T_v = \mu dx/dt$ , for elastic media  $T_{el} = G_e x$ , and for plastic elements  $dx/dt = 0$ , for  $|T_p| < G_p$ , and  $|T_p|$  does not exceed the yield stress  $G_p$  (i.e., the plastic element yields for specific torques equal to the yield stress, is rigid for torques less than the yield stress, and cannot support any torque greater than the yield stress). The simplest model (which is to say the one with the fewest elements) that appears to satisfy the above four conditions is a serial arrangement of a parallel viscoplastic element and a parallel viscoelastic element. This mechanical arrangement is shown in Fig. 2. Note that this model has elements in common with other rheological models of biological materials including the standard viscoelastic solid (see, e.g., Schmid-Schönbein et al., 1981). The elastic modulus and viscosity of the viscoelastic element are denoted  $G_e$  and  $\mu_e$ , respectively. The yield stress and viscosity of the viscoplastic element are denoted  $G_p$  and  $\mu_p$ , respectively.

Also shown in Fig. 2 are the angular displacements of the elements, for which we adopt the following conventions. Let  $\vartheta$  be the overall measured angle (cf. Eq. (1)),  $\alpha$  the angular displacement of the viscoplastic component, and  $\phi$ , the angular displacement of the viscoelastic component. These components being in series then implies

$$\vartheta(t) = \phi(t) + \alpha(t).$$

We choose the origin of time and the zeros of the angular coordinates as follows. The initial step in twisting field from 0 to  $B_{tw}$  occurs at time  $t = 0$ . At that time,

$$\vartheta(0) = \phi(0) = \pi/2 \quad \text{and} \quad \alpha(0) = 0.$$

3.1. *The equations of motion for the unified model*

These fall into the three time periods, reflecting respectively (I) the time before the onset of the twisting field, (II) the time during which the twisting field is on, and (III) the recovery time following the cessation of the twisting field. These periods are divided by the time points  $t = 0$  (separating Period I—Baseline and Period II-Twist) and  $t = t_{\text{off}}$  (separating Period II-Twist and Period III-Recovery).

*Period I-Baseline,  $B_{\text{tw}}$  off.  $t \leq 0$ .*  $T$  is zero, and there is consequently no displacement of any of the elements. In particular,  $\phi$ ,  $a$ , and  $\vartheta = a + \phi$  are constant at their initial values; thus

$$\left. \begin{aligned} \alpha(0) &= 0, \\ \phi(0) &= \pi/2, \\ \vartheta(0) &= \pi/2. \end{aligned} \right\} \tag{3}$$

*Period II-Twist,  $B_{\text{tw}}$  on.  $0 < t < t_{\text{off}}$ .* Twisting field =  $B_{\text{tw}}$  for  $0 < t < t_{\text{off}}$ , and typically  $t_{\text{off}} = 60$  sec. The equations of motion for this period subdivide into at most two sub-periods depending on whether the plastic element is yielding or not. In particular, if  $c B_{\text{tw}} \sin(\vartheta) \leq G_p$ , then there is no slipping, and  $d\alpha/dt = 0$ . By contrast, if  $c B_{\text{tw}} \sin(\vartheta) > G_p$  then the plastic element yields, and  $d\alpha/dt < 0$ . Call the two sets of equations of motion respectively “slip” and “noslip”. The time interval over which each is applicable is given by, respectively,  $0 < t \leq t_1$  and  $t_1 < t \leq t_{\text{off}}$ . The transition time  $t_1$  is determined as follows. If  $c B_{\text{tw}} \leq G_p$ , then “noslip” applies for  $0 < t \leq t_{\text{off}}$ . In this case define the transition time  $t_1$  to “noslip” by  $t_1 = 0$ . If  $c B_{\text{tw}} > G_p$  then “slip” applies for  $0 < t < \min(t_1, t_{\text{off}})$ , followed by “noslip” for  $t_1 < t \leq t_{\text{off}}$  if  $t_1 < t_{\text{off}}$  and where  $t_1$  is defined implicitly by  $6(t_1) = \sin^{-1}(G_p/cB_{\text{tw}})$ . Note that the computation of  $\vartheta(t)$  past  $t = t_{\text{off}}$  need not be done for this implicit determination of  $t_1$ , since only  $\min(t_1, t_{\text{off}})$  is needed; in this case the uncomputed  $t_1$  is taken as  $> t_{\text{off}}$ .

*Period II-Twist, “Slip”:* Equations of “slip” motion (total torque/vol applied is the same across both the viscoelastic and viscoplastic elements since they are in series):

$$\left. \begin{aligned} cB_{\text{tw}} \sin(\vartheta) &= G_c(\pi/2 - \phi) - \mu_e d\phi/dt, \\ &= G_p - \mu_p d\alpha/dt, \\ \vartheta &= \phi + \alpha, \end{aligned} \right\} \tag{4}$$

with initial conditions, by continuity, equal to the final conditions above in **Eq.** (3). Note that for a positive  $T$  all of the terms contributing to  $B_{\text{tw}} \sin(\vartheta)$  are also positive, i.e.,  $d\phi/dt$  and  $d\alpha/dt$  are both negative.

*Period II-Twist, “Noslip”:* Equations of “noslip” motion (total torque/vol applied is the same across both the elements as before, but is less than the yielding stress  $G_p$ ) are given by:

$$\left. \begin{aligned} c B_{tw} \sin(\vartheta) &= G_e(\pi/2 - \phi) - \mu_e d\phi/dt, \\ d\alpha/dt &= 0, \\ \vartheta &= \phi + \alpha, \end{aligned} \right\} \quad (5)$$

with initial conditions given by continuity with the final angles from Period II-Twist, "Slip":

$$\left. \begin{aligned} \alpha(t_1) &= \alpha(t_1^-), \\ \phi(t_1) &= \phi(t_1^-). \end{aligned} \right\} \quad (6)$$

*Period III-Recovery*,  $B_{tw}$  off.  $t_{off} < t$ . The twisting field is back to zero. The equations of motions are given by

$$\left. \begin{aligned} 0 &= G_e(\pi/2 - \phi) - \mu_e d\phi/dt, \\ 0 &= d\alpha/dt, \\ \vartheta &= \phi + \alpha, \end{aligned} \right\} \quad (7)$$

the same as in  $t \leq 0$  (Period I-Baseline, Eq. (3)), but with initial conditions being given by continuity at  $t = t_{off}$ ,

$$\left. \begin{aligned} \alpha(t_{off}) &= \alpha(t_{off}^-), \\ \phi(t_{off}) &= \phi(t_{off}^-). \end{aligned} \right\} \quad (8)$$

### 3.2. Solutions to the equations of motion

*Period II-Twist*.  $0 < t < t_{off}$ . There is no analytic solution expressible in terms of the elementary transcendental functions for the equations of motion given by Eqs. (4) and (5). These must therefore be solved numerically; we used fourth order Runge-Kutta (Press et al., 1986) technique in two dependent variables ( $\alpha$  and  $\phi$ ).

*Period III-Recovery*.  $t_{off} < t$ . Here the equations of motion (Eq. (7)) are linear, and the solution is immediate:

$$\left. \begin{aligned} \alpha(t) &= \alpha(t_{off}), \\ \phi(t) &= \pi/2 + (\phi(t_{off}) - \pi/2)e^{-(t-t_{off})/\tau}, \\ \vartheta(t) &= \alpha(t) + \phi(t), \end{aligned} \right\} \quad (9)$$

where the time constant  $\tau$  is given by the viscosity to stiffness ratio,  $\tau = \mu_e / G_e$ .

## 4. Rheological Models and Parameter Estimation-Current Techniques

*Stiffness*: The quantitative estimation of stiffness is typically computed as the ratio of the specific torque at 60 sec,  $T(60)$ , divided by some estimate of strain at that time. The strain is typically taken to be the angular rotation at 60 sec,  $\vartheta(60)$ , relative to the angle at  $t = 0$  ( $n/2$ ).

However, the presence of incomplete angular recovery implies that the strain at  $t = 60$  is ambiguous. That is, there are two angles that may be associated with the zero stress state, the initial angle ( $n/2$ ) and the asymptotic angle seen at the end of the recovery period ( $\vartheta(\infty)$ ), and therefore the angular strain at  $t = 60$  is multiply defined, and could be taken as either  $n/2 - \vartheta(60)$  or  $\vartheta(\infty) - \vartheta(60)$ . The former is nearly universally used, but in order to compensate in part for the difficulties associated with nonrecoverable deformation, Butler et al. (1992) also suggested using the latter definition of strain; this was subsequently used by Tagawa et al. (1997) (see the differences between Figs. 3 and 5, which used the former definition, and Fig. 4 which used the latter). If there is relatively complete angular recovery, and if there is an approximate angular plateau, then this is not a problem. Thus, Zaner and Valberg (1989) successfully estimated the effect of actin binding proteins on the stiffness of actin gels. By contrast, if there is little recovery, then the strain computed as the angular rotation relative to  $t = 0$  ( $n/2 - \vartheta(60)$ ) is clearly in error. In the extreme case of a pure viscous fluid for which the stiffness is actually zero, the stiffness computed as  $T(60)/(\pi/2 - \vartheta(60))$  is totally artifactual.

Since the cell's mechanical response to an externally applied stress is clearly not that of a simple spring, a second issue is the choice of whether to associate the computed stiffness at  $t = 60$  with the rotation or stress at particular times in order to characterize the effects of a variety of perturbations. For example, Wang et al. (Potard et al., 1997; Wang and Ingber, 1994; Wang and Ingber, 1995) plotted stiffness versus the initial stress  $T(0)$ . They showed a systematic change in the stiffness with initial stress from which they inferred the existence of a stiffening response and the presence of prestress in the cell; however, the quantitative characterization of such a response is necessarily in error, since the stiffness was not characterized as a function of the stress at the time the stiffness was estimated. Potard et al. (1997) plotted stiffness both against  $T(0)$  and the rotation at the same time,  $n/2 - \vartheta(60)$ . They used these data to argue that in confluent epithelial cells, there was little evidence for prestress.

*Viscosity:* By the arguments presented above, in a purely viscous medium  $d\vartheta/dt$  bears a simple proportional relation to the applied stress. This led several investigators (Bizal et al., 1991; Valberg and Feldman, 1987; Zaner and Valberg, 1989) to use the formulation of Valberg and Butler (1987) to estimate cytoplasmic viscosity. Just as the methods of estimating stiffness given above ignore the effects of viscosity, so too this method of estimating viscosity ignores the effects of elasticity. Since there is substantial angular recovery in virtually all preparations studied, it follows that a correspondingly large fraction of the stress is borne by elastic elements. Forcing the data into a formulation wherein the stress is borne entirely by viscosity therefore leads to systematic overestimates, by several orders of magnitude, of the numerical values of the viscosity (see below).

A second method of obtaining estimates of viscosity is by combining an estimate of stiffness from Period II-Twist with an estimate of the time constant for angular recovery seen in Period III-Recovery. This suffices to estimate the viscosity under the assumption of a parallel viscoelastic medium, since the time constant for the exponential recovery of angle is given by the ratio of the viscosity to the elastance. This method was introduced in studies of frog oocytes and eggs (Butler et al., 1992; Kelly, 1992) and of cultured cells (Tagawa et al., 1997; Wang and Ingber, 1995; Wang and Ingber, 1994). To the extent that there is relatively complete recovery

### Macrophages

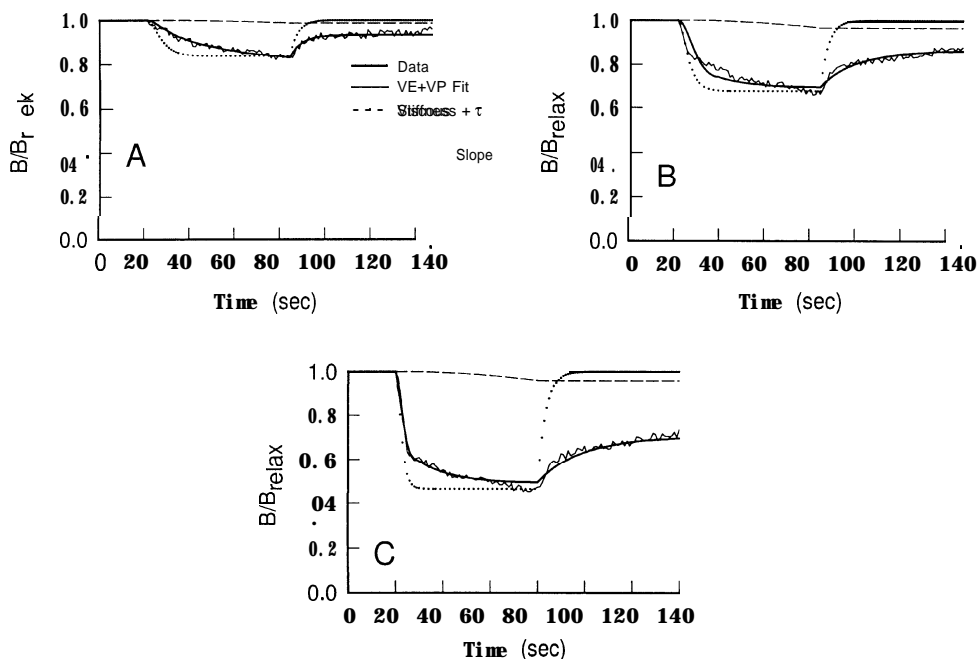


Fig. 3. Data digitized from Bizal et al. (1991). Cells exposed to 3 different twisting field strengths; Panel A, 1.25 mT; Panel B, 2.5 mT; Panel C, 5.0 mT. Results of the 3 different methods of analysis are also plotted as the indicated lines. Here, and in Figs. 4 and 5, note that only the VE+VP Fit approximates the complete data curves, including both twisting and recovery.

### Cardiocytes

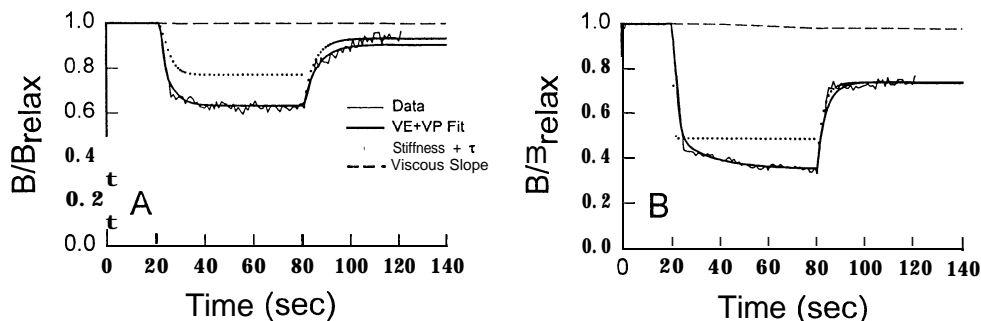


Fig. 4. Data digitized from Tagawa et al. (1997). Hypertrophied myocytes studied at baseline, Panel A and after exposure to colchicine, Panel B. Results of the 3 different methods of analysis are plotted as in Fig. 3. Note that for the Stiffness+ $\tau$  method,  $\vartheta(\infty)$  has been taken as the zero stress state, and that therefore the stiffness is computed from the angular strain at one minute given by  $\vartheta(\infty) - \vartheta(60)$ . This accounts for the adequate fit during recovery, but at the cost of a very poor fit during twisting, and a discontinuity at 1 minute. This phenomenon is the complement of similar problems seen in Figs. 3 and 5, where the fit during recovery is very poor.

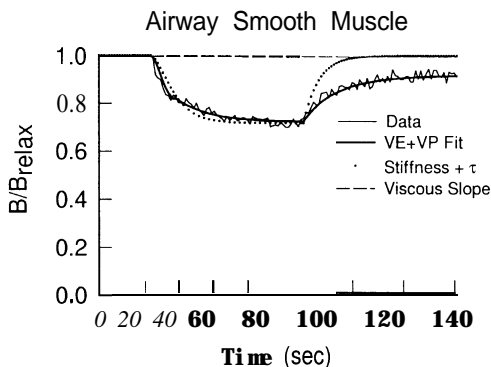


Fig. 5. Data digitized from Hubmayr et al. (1996). Results of 3 different methods of analysis are also plotted as in Fig. 3.

and that an angular plateau has been approximately reached during the twisting period, then this method has some merit. However, the continued presence of some stress being borne by viscous elements at the end of the twisting period and the lack of full recovery in fact compromises this method.

## 5. Results

We compared our viscoelastic-viscoplastic model to several methods currently in use to characterize the rheological properties of cells. We chose to analyze data already in the literature, comprising three different cell types: macrophages (three separate twisting field strengths) (Fig. 3 A, B, C), hypertrophied right ventricular cardiocytes (baseline and after treatment with colchicine) (Fig. 4 A, B), and human airway smooth muscle cells (Fig. 5). Note also that in the case of the macrophage data, the particles have been phagocytized and are therefore intracellular, whereas the particles in both the cardiocyte and smooth muscle cells have been ligand coated and are membrane bound extracellularly. Data for each analysis were obtained by digitizing the actual published twist ( $B(t)$ ) and no-twist ( $B_{\text{relax}}(t)$ , or “relaxation”) data curves. Following the ideas of Valberg and Feldman (1987), we then normalized for relaxation by taking  $\vartheta(t)$  to be the ratio  $B(t)/B_{\text{relax}}(t)$ . (See Section 6 for problems with this approach.) These data are shown redrawn as the thin solid line in the figures. For each data set we computed the following.

*Stiffness+ $\tau$  method:* In this method (Butler et al., 1992; Kelly, 1992; Wang and Ingber, 1995; Wang and Ingber, 1994) the stiffness is calculated either as the ratio  $T(60)/(\pi/2 - \vartheta(60))$  in Figs. 3 and 5, or as the ratio  $T(60)/(\vartheta(\infty) - \vartheta(60))$  in Fig. 4. These choices were made based on the actual methods used by these authors. The data during Period III-Recovery are assumed to be described by a parallel viscoelastic element, whose viscosity is estimated by the ratio of that stiffness to  $\tau$ , where  $\tau$  is the time constant for the exponential recovery during Period III-Recovery. The solution to the equations of motion for a parallel viscoelastic body with those values of stiffness and viscosity are plotted as the dotted lines in the Figs. 3-5. Note

however, that the initial angle for the recovery period in Fig. 4 is determined by the final angle observed during twisting, and hence there is a discontinuity in the model's response at 60 sec.

*Viscous Slope method:* In this method (Bizal et al., 1991; Valberg and Feldman, 1987; Zaner and Valberg, 1989) stiffness is not considered. The viscosity is estimated from the average slope  $d\vartheta/dt$  over the last 20 sec of Period II-Twist and the equation defining a single viscous element  $T_v = B_{tw} \sin(\vartheta) = -\mu d\vartheta/dt$ . However, because the experimental data approach a plateau, the slopes are very low and therefore the computed viscosity values are very high. As a result, the solution to the equations of motion for a pure viscous medium with those values of viscosity generate curves of  $B(t)/B_{relax}(t)$  that are virtually indistinguishable from the initial value of unity. These results are plotted as the dashed line in the figures. Bizal et al. (1991) acknowledged that a portion of the rotation was due to elastic elements in parallel or to elastoplastic elements in series, but did not quantify it.

*VE+VP Fit method:* The equations of motion (Eqs. (4) and (5) for Period II-Twist and Eq. (7) for Period III-Recovery) for the viscoelastic-viscoplastic model proposed here were numerically solved, and the four parameters were determined by the criterion of minimizing the squared residuals of the fit to the data  $B(t)/B_{relax}(t)$ . This best fit curve is plotted as the heavy solid line in the figures. (It is important to note that the presence of the factor  $\sin(\vartheta)$  in the equations of motion during the twist makes the governing equations nonlinear, and no analytic solution exists in terms of elementary transcendental functions.)

Inspection of the three simulations across all cell types and all conditions reveals several common features. First, it is true by definition that the Stiffness+t method, since it is a parallel viscoelastic model, must display complete angular recovery following cessation of the twisting field if the initial angle during recovery is not artificially set. This is seen in Figs. 3 and 5, where we note that the original data systematically show a lack of full recovery. The reset of the initial angle during recovery and the fit to only that portion of the data in Fig. 4 accounts for the goodness of fit there. On the other hand, having fit the recovery period implies that the fit during the twisting period is correspondingly very poor. In the case of the Viscous Slope method, the simulated curves are faithful to the data in neither Period II-Twist nor Period III-Recovery. Unlike the previous method, the Viscous Slope method does exhibit angular loss. However, the presence of the near plateau in the actual experimental data leads to extremely high viscosity values, and therefore only a very small amount of angular loss. By contrast with either of these two methods, it is clear that the VE+VP method proposed here provides a strikingly good fit to the data curves for all three cell types and under all conditions. The important feature of this model is that it fits the data adequately and consistently across the entire experimental time period.

The parameters recovered from the three methods described above are given in Table 1. Entries denoted by R are those actually reported in the respective cited reference. The remaining numbers are values obtained by our calculations using the stated methods as described above. The following features are of note. First, the numerical values of the viscosities given by the Viscous Slope method are extremely high compared with the viscosities estimated by the other two methods. Second, note that the changes in macrophage viscosity with field strength and the change in cardiocyte stiffnesses with colchicine treatment are similar among the methods.

Table 1  
Dependence of parameter values on analysis method

	Macrophages <sup>1</sup>			Cardiocytes <sup>2</sup>		Smooth muscle cells <sup>3</sup>
	$B_{tw} = 1.25$ mT	$B_{tw} = 2.5$ mT	$B_{tw} = 5.0$ mT	Baseline	Post colchicine	
				$B_{tw} = 3$ mT	$B_{tw} = 3$ mT	
Viscous slope						
Visc. (poise)	R: 17,500	R: 29,000	R: 45,000	6 1,000	4,800	59,000
Stiffness+ $\tau$						
E (dyn/cm <sup>2</sup> )	70	70	80	R: 20	R: 7	R: 140
Visc. (poise)	420	480	510	R: 90	R: 20	860
VE+VP						
$G_e$ (dyn/cm <sup>2</sup> )	170	230	330	22	10	160
$G_p$ (dyn/cm <sup>2</sup> )	37	67	110	11	5	66
$\mu_e$ (poise)	1050	4000	7000	153	55	2700
$\mu_p$ (poise)	630	330	360	23	77	170

R: Denotes those values as reported in the cited references.

Data obtained from: <sup>1</sup>Bizal et al., 1991; <sup>2</sup>Tagawa et al., 1997; <sup>3</sup>Hubmayr et al., 1996.

## 6. Discussion

We wish to emphasize that all methods of characterizing rheological data rest on implicit or explicit models. The extreme cases of pure elastic and pure viscous media have been treated before, but it is essential that for media that display both elastic and viscous properties, and that perhaps include yielding as well, the models used be self-consistent. Thus, it is problematic to analyze the exact same set of data with two incompatible models (e.g., purely elastic with full recovery and purely viscous with zero recovery) to estimate both elastic moduli and viscosities. Furthermore, even if, e.g., only the viscosity is to be measured, the presence of cytoplasmic elasticity will tend to retard the strain rate of the medium in response to any given torque, and so will masquerade as an apparent increased viscosity. This is seen in the markedly elevated estimates of viscosity made by Bizal et al. (1991) (Table 1). Similarly, the presence of viscous or plastic elements in series leads to the commonly observed lack of full recovery, and therefore contribute to an artifactually low value of the stiffness, reported by Wang and Ingber (1994, 1995), and Hubmayr et al. (1996). This is particularly important insofar as dissipative and energy storage mechanisms are linked at the molecular level, and separating these effects is made all the more difficult when each can mimic the other within the classical model frameworks. Specifically, one may examine the effect of a variety of interventions (e.g., drugs, temperature, state of cell spreading) in terms of a particular rheological parameter, but the ambiguities associated with its estimate by current techniques compromise the degree

to which specific alterations in cytoplasmic or cytoskeletal mechanics can be identified. Our attempt in this work has been to put forth a model which simultaneously deals with all of the major features displayed in actual data curves, thus avoiding the problem of inconsistency. There may of course be other models, especially those with more than four discrete elements or even with distributed elements, that fit particular data sets equally well or better, but of those with a maximum of four elements, the model proposed here seems to adequately characterize the observations.

Inspection of Table I shows a number of features that link the four parameters of the VE+VP Fit model with the stiffness and viscosity estimated by the Stiffness+ $\tau$  method. The stiffness is usually less than our estimate of  $G_e$ . This is not surprising for two related reasons. First, as remarked above, the failure to observe full recovery implies a lower value for the estimated stiffness, and second, our VE element is (by design) in series with an element that can account for the nonrecovery. Structurally, the non rate dependent features of the VE element and the VP element are in series, and therefore any estimate of an "equivalent" stiffness is necessarily lower. Note that this is only a qualitative argument, because the extent to which the plastic element yields varies with field strength, and so its contribution to the lowered apparent stiffness cannot be simply quantified. Nevertheless, the values seen in Table 1 for stiffness,  $G_e$ , and  $G_p$  do show the expected qualitative relationship. Finally, Tagawa et al. (1997) accounted for nonrecovery in their analysis of stiffness, using  $\vartheta(\infty)$  as the rotation angle corresponding to zero stress, and hence  $\vartheta(\infty) - \vartheta(60)$  as the angular strain at 1 minute. This is the second method of defining stiffness described above in Section 4. Since this includes just the recovery period, during which only  $G_e$  contributes elastically in our model, it is not surprising that their stiffness values are nearly identical to our calculated  $G_e$ .

Similarly, the numerical values of the viscosity (determined by the Stiffness+ $\tau$  method) also show the same features when compared with our estimates of  $\mu_e$  and  $\mu_p$ . Thus, all estimates of the viscosity by using stiffness and  $\tau$  are systematically lower than  $\mu_e$ . As above, the extent to which  $\mu_p$  contributes as a series viscosity depends on the extent to which the plastic element yields. It follows that, while not simply quantifiable, the relationships among the viscosity thus determined and  $\mu_e$  and  $\mu_p$  are what are to be expected when all dissipation is lumped into a single viscosity manifested through a single time constant. By contrast, as noted above, the estimates of viscosity given by using the slope  $d\vartheta/dt$  over the latter portion of the twisting period are extremely high due to the presence of an approximate plateau (which we interpret as being elastically supported). The fact that the simulated  $B(t)/B_0$  for a purely viscous medium with those viscosities show only a very small departure from 1.0 strongly suggests that this method is not appropriate for the estimate of viscosity. Nevertheless, it is interesting to note that the observation of shear thickening in macrophages with increasing shear stress, as originally reported by Bizal et al. (1991), remains valid when the data are re-analyzed in the self consistent manner proposed here (compare the entries in Table 1 for the macrophages at different field strengths).

Despite the strikingly good fits displayed by the VE+VP Fit method, shown in Figs. 3-5, it is nevertheless important to identify at least some of the model's potential major limitations. The most important one is that we explicitly assume ideal elastic, plastic, and viscous elements, characterized by  $G_e, G_p, \mu_e$ , and  $\mu_p$ . If the elements were ideal, then these values would be constants, and recovered estimates of these would not depend on the probing field strength.

Table 1 shows that, at least for macrophages, this is not true. This is not unexpected, insofar as virtually all biological materials display nonlinearities in both their elastic and viscous properties. Nevertheless, it is true that for a given run in a given preparation, the VE+VP Fit representation is surprisingly faithful to the data. Another limitation is the possibility of data for which this model does not give a good fit. While this may indeed occur in some cell types or with some interventions, the published curves taken from three different cell types that we have analyzed by this method do not suggest such a likelihood.

While the general features (1)–(4) listed in Section 3 were the origin of the construction of the VE+VP Fit model, it is important to appreciate its versatility in terms of particular submodels. For example, one submodel may have a zero yield stress (absence of the plastic element). In this case, there will be no plateau during twisting, while the presence of partial recovery is preserved. This is indeed observed in some cell populations. In particular, twists of longer durations can sometimes reveal such a failure of a plateau to develop (Butler et al., 1992; Zaner and Valberg, 1989). As a second example, the studies of Zaner and Valberg (1989) on F-actin with and without actin binding proteins showed curves with essentially full recovery, and with very sharp transitions when the twisting field was turned on and off. This is the elastic submodel characterized by negligible viscosity and a yield stress greater than the initial specific torque.

There is one additional feature of the observed data which needs to be addressed. All cell types show, in greater or lesser extent, a systematic decline in the remanent magnetic field even in the absence of twisting. This phenomenon, called “relaxation”, is well-known, and is due to particle re-orientation due to a wide variety of possible mechanisms, including intracellular motion, Brownian motion of thermal origin, cytoskeletal re-organization, internalization of membrane bound particles, etc. The effect of twisting the particles is thus superposed in some sense on this continuing underlying biological process. It is unknown how these phenomena are coupled. Valberg and Feldman (1987) proposed a method for “normalizing” the observed  $B(t)$  curve during and after twisting protocols by arguing that with no twist, the observed  $B_{\text{relax}}(t)$  can be thought of as viewing the particles from a rotating coordinate system. They concluded the ratio  $B(t)/B_{\text{relax}}(t)$  is a corrected version of the remanent field, and represents that additional drop in  $\sin(O)$  directly attributable to twisting. To our knowledge, all previous work, including this paper, has taken this corrected remanent field  $B(t)/B_{\text{relax}}(t)$  as the measurement of  $\sin(O)$ . However, the argument that the effects of twisting and relaxation can be superposed in this fashion is not valid, because the distribution of particle orientations due to relaxation implies that there is a corresponding distribution of torques applied by the twisting field. Even assuming that the increasing spread of the angular distribution due to relaxation is unaffected by twisting (which is not known), it is an open question how to recover the equivalent remanent field behavior due to twisting alone. This is an especially important question for future progress in the rheological assessment of those cell types that display a significant amount of relaxation over the course of minutes.

Despite the fact that the rheological model proposed here shows a remarkably faithful fit to observed data, the assignment of parameter values to specific cellular elements remains open. The cytoskeletal polymers F-actin, intermediate filaments, and microtubules will certainly contribute to the elastic elements in the model, as will the mechanical properties of cell surface receptors when probed with membrane bound beads, but which of these is associated

with the viscous component and which with the plastic or yielding component remains to be determined. This could presumably be addressed through the interventions of selective cytoskeletal disruptors and independent measurements of the mechanical properties of specific receptors. Of particular interest would be, for example, the possibility that the viscosity is not a strictly fluid viscosity, but rather represents the re-organization of at least one of the cytoskeletal polymers through its depolymerization and re-polymerization in response to the stress conferred by the twisting magnetic particle. This presumably leads to an energy loss, and is thus a logical candidate for a coupling between the viscosity and elastic parameters  $\mu_e$  and  $G_e$ . This coupling of the parameters at the molecular level of the cytoskeleton can also be interpreted as one of the origins of the yielding phenomenon in response to externally imposed strains (Janmey et al., 1991).

In summary, we have developed a self-consistent rheological model that faithfully describes the observed behavior of both intracellular and membrane bound extracellular ferromagnetic particles when twisted magnetometrically, in several different cell types, with different twisting torques, and with different drug administrations. It captures all of the essential features of the complete data set, and provides parameters that can be interpreted in terms of classical elastance, viscosity, and plasticity. This model now allows us to unambiguously, in the sense that dissipative and elastic contributions are not confounded, probe the mechanistic origins of a variety of cell properties including differential functions of the elements comprising the cytoskeleton as well as their interaction with the extracellular matrix through specific receptors.

## Acknowledgments

We would like to acknowledge Dr S. Mijailovich for initial help in the numerical implementation of the programs required. We also especially thank Drs N. Wang and J. Fredberg for stimulating discussions. This study was supported by grant R41 CA64964 from the National Institutes of Health. Dr S. Kelly was supported by the Medical Research Council of Canada and the Canadian Lung Association.

## References

- Bizal CL, Butler JP, Valberg PA. Viscoelastic and motile properties of hamster lung and peritoneal macrophages. *J. Leukoc. Biol.*, 199 1;50:240–25 1.
- Butler JP, Kelly SM, Miki H, Rogers R. Rheology and spontaneous oscillations in *Xenopus* oocytes and eggs. *FASEB J.*, 1992;6:A4003.
- Fong JH-J. *Mechanochemical Transduction Across Integrin Receptors*. Cambridge: Harvard; 1996.
- Hubmayr RD, Shore SA, Fredberg JJ, Planus E, Panettieri Jr RA, Moller W, Heyder J, Wang N. Pharmacological activation changes stiffness of cultured human airway smooth muscle cells. *Am. J. Physiol.*, 1996;271:C1660–C1668.
- Janmey PA, Euteneuer U, Traub P, Schliwa M. Viscoelastic properties of vimentin compared with other filamentous biopolymer networks. *Journal of Cell Biology*, 199 1; 113: 155-160.
- Kelly SM. *Cell Mechanical Properties and Volume Control*. PhD Thesis. Montreal, Quebec, Canada: Department of Experimental Medicine, McGill University; 1992.

- Lamontagne D, Pohl U, Busse R. Mechanical deformation of vessel wall and shear stress determine the basal release of endothelium-derived relaxing factor in the intact rabbit coronary vascular bed. *Circ. Res.*, 1992;70:123-130.
- Lien DC, Hensen PM, Capen RL, Henson JE, Hanson WL, Wagner Jr WW. Neutrophil kinetics in the pulmonary microcirculation during acute inflammation. *Lab. Invest.*, 1991; 65: 145-159.
- Potard USB, Butler JP, Wang N. Cytoskeletal mechanics in confluent epithelial cells probed through integrins and E-cadherins. *Am. J. Physiol.*, 1997;272:C 1654-C 1663.
- Press WH, Flannery SA, Teukolsky SA, Vetterling WT. *Numerical Recipes: The Art of Scientific Computing*. Cambridge, UK: Cambridge Univ. Press; 1986.
- Schmid-Schönbein GW, Sung KL, Tozeren H, Skalak R, Chien S. Passive mechanical properties of human leukocytes. *Biophysical Journal*, 1981;36(1):243-256.
- Tagawa H, Wang N, Narashige T, Ingber DE, Zile MR, Cooper IV G. Cytoskeletal mechanics in pressure-overload cardiac hypertrophy. *Circ. Res.*, 1997;80:281-289.
- Valberg PA, Butler JP. Magnetic particle motions within living cells: physical theory and techniques. *Biophys. J.*, 1987;52:537-550.
- Valberg PA. Magnetometry of ingested particles in pulmonary macrophages. *Science*, 1984;224:513-516.
- Valberg PA, Albertini DE. Cytoplasmic motions, rheology, and structure probed by a novel magnetic particle method. *J. Cell Biol.*, 1985;101:130-140.
- Valberg PA, Butler JP. Intracellular movement and intracellular viscosity: What can magnetic microparticles tell us? *Comments Theor. Biol.*, 1990;2:75-97.
- Valberg PA, Feldman HA. Magnetic particle motions within living cells. Measurement of cytoplasmic viscosity and motile activity. *Biophys. J.*, 1987;52: 551-561.
- Wang N, Butler JP, Ingber DE. Mechanotransduction across the cell surface and through the cytoskeleton. *Science*, 1993;260: 1124-1127.
- Wang N, Ingber DE. Probing transmembrane mechanical coupling and cytomechanics using magnetic twisting cytometry. *Biochem. Cell Biol.*, 1995;73:327-335.
- Wang N, Ingber DE. Control of cytoskeletal mechanics by extracellular matrix, cell shape, and mechanical tension. *Biophys. J.*, 1994;66:2181-2189.
- Wirtz HRW, Dobbs LG. Calcium mobilization and exocytosis after one mechanical stretch of lung epithelial cells. *Science*, 1990;250: 1266-1269.
- Worthen GS, Schwab III B, Elson EL, Downey GP. Mechanics of stimulated neutrophils: Cell stiffening induces retention in capillaries. *Science*, 1989;245: 183-186.
- Zaner KS, Valberg PA. Viscoelasticity of F-actin measured with magnetic microparticles. *J. Cell Biol.*, 1989;109:2233-2243.